OXFORD JOURNAL
OF STUDENT
SCHOLARSHIP

Which Variable Renewable Serves Pakistan's Binding Hour? Metered Evidence After the Peak Moved to the Evening

Sheraz Hassan, Muhammad Sami Shahid
sherazhassan765@gmail.com, samishahid7623@gmail.com

ABSTRACT

Pakistan's contracted generating capacity is approximately 32% higher than its peak demand. We analyzed peak demand by reviewing hourly system operator data for fiscal years 2016-2025. In fiscal year 2025, the hour with the highest demand moved from 14:00 to 23:00. The data further indicated that 90% of the 50 binding hours (the highest demand hours of the year) occurred in the evening, up from 32% the year before. This shift is associated with the greater use of distributed solar power, which reduced the demand the operator sees during the day. Solar power does not generate at night; wind power's capacity factor for the 50 binding hours was 0.504, and 0.239 for the year. Utility-scale solar had a capacity factor of 0.024 for those hours and 0.191 for the year.

In the May to September season of fiscal year 2025, wind's hourly output was correlated with demand at +0.317, and utility solar's at −0.347. A three-factor decomposition, which takes into account month and hour of the day, shows wind's advantage comes mostly from the season, not hour of the day. In both years, the highest demand days were also windier than other days of the same month at the same hour. Monsoon wind output typically changes by 25-33% between years. Allowing generously for unrecorded wind curtailment does not change the comparison with solar. Because some rationing goes unrecorded, the recorded values are likely a lower bounding estimate.

Adding estimated distributed solar back to the demand value, with capacity held constant, moves the binding hours back to the afternoon and raises solar's peak-coincidence ratio from 0.124 to 2.6-3.4, partly by construction. Solar's ranking in Pakistan's planning models may therefore reflect the demand curve before distributed solar spread.

Keywords: *capacity value; peak coincidence; wind power; distributed solar; peak demand; monsoon; Pakistan electricity planning*

1. INTRODUCTION

Fiscal year (FY) 2025 saw the contracted capacity of Central Power Purchasing Agency (Guarantee) Limited (CPPA-G) stand at 38,431 MW with a peak demand of 29,201 MW, leaving a margin of 31.6 percent (1). However, load shedding is common in Pakistan. The main reasons stated for load shedding

include limitations of the electricity transmission system, circular debt, and the shortfall of the capacity available to meet the demand. Some of it is also applied for commercial reasons, to feeders with high losses (Section 4.5). This paper does not test why load shedding occurs. It asks a narrower question about adequacy: at which hours the system is now most stretched, and which variable renewable produces at those hours.

In FY2025, the reserve margin changed due to reasons unrelated to the actual demand. The contracted capacity stood at 42,512 MW at the beginning of the fiscal year and fell by 4,081 MW to 38,431 MW (1). The contract for Guddu's 1,015 MW plant expired. Thermal capacity contracted from independent power producers fell by 3,931 MW, mainly because six power purchase agreements totaling 2,829 MW were terminated and the 1,600 MW Kot Addu Power Company (KAPCO) plant, whose contract expired in October 2022, was removed apart from 550 MW reinstated in June 2025. Hydel capacity rose by 865 MW, mostly from the new 884 MW Suki Kinari plant (1). In the same year, the hour of peak demand shifted from 14:00 to 23:00. The solar power plants produce no electricity at night; therefore, all the peak demands falling at night get no solar power. The share of the 50 highest-demand hours falling after the setting of the sun increased from 32 to 90 percent. Season does not explain this change, because every year's highest-demand hours fall between May and September.

The migration was associated with one of the quickest deployments of distributed solar. Over the period, solar PV module imports grew from 0.76 GW in 2017 to an estimated 16.62 GW in 2024. By August 2025, total module imports reached about 50 GW, and module prices fell to about 0.08 USD/W (2). By June 2025, based on import data, the total distributed solar capacity reached about 38 GW with Renewables First forecasting 51 GW for the financial year 2025/26 (3, 4). Solar's contribution to the total electricity generated also rose from about 10% in FY2023 to about 28% in FY2025 (3). Much of this capacity is invisible to the system operator, and shows up only as a lack of system demand. Other changes over the same years, such as higher tariffs, shifts in industrial demand, hotter nights and changes in how load management is recorded, could also move the peak; Section 4.1 considers them.

1.1 How Pakistan's Electricity Future Has Been Modeled

Pakistan's scenarios and plans consistently place solar PV before wind. In the LUT Energy System Transition model, the power sector scenario returns solar at 92.7% of installed capacity (5), and at 88% in a later, cross-sector scenario (6). Long Range Energy Alternatives Planning (LEAP) models for 2015-2050 maintain this same ordering on lowest net present cost (7, 8). Other models, including MESSAGE (9) and EnergyPLAN (10) as well as a range of other least-cost planning studies (11-14), also corroborate this same prioritization of solar PV. Additionally, hourly-based integrated models of the region corroborate this priority (15). The Indicative Generation Capacity Expansion Plan adopts a cost-minimizing approach to meet projected demand (16). The 2024-34 plan was developed in PLEXOS and so satisfies reliability only as a loss of load or reserve-margin constraint (17). These approaches validate solar prioritization on cost. Sadiqa and colleagues mention that the better wind resource along the coasts of Sindh and Balochistan, being far from the main consumption centers, contributes to the

prioritization of solar over wind, as solar is more widely distributed (6). This is also supported by the levelized cost of energy.

1.2 Capacity Value

None of the models we reviewed examine what each resource provides during the peak demand hours. This value is known as capacity credit or effective load carrying capability and has been defined and discussed in the literature. Garver defined it in 1966 and concentrated the calculation on the high risk hours (18). After that, Keane and others established the loss-of-load-expectation (LOLE) method as the preferred approach (19). Capacity factor during peak hours (CFPH) is used as a surrogate (20, 21). Operators have implemented these concepts in their practices. Wind and solar resources are accepted to have an effective load carrying capability by the Midcontinent Independent System Operator (MISO) using about 30 years of hourly resource and load data (22). The ISO New England (ISO-NE) has set a target for an annual loss of load expectation of 0.1 day, and applies effective load carrying capability in this context (23). Planners in Pakistan do not assess effective load carrying capability from domestic data in their plans. In LEAP models, where a capacity credit is given at all, it is an availability factor taken from studies of other systems, so it does not depend on timing (8). To the best of our knowledge, no published Pakistani energy model assesses effective load carrying capability from domestic hourly data.

1.3 Pakistan's Wind Resource and the Monsoon

It is unlikely that the impact of this omission will be the same for both of the technologies. As of 30 June 2024 and 2025, the total wind capacity of Pakistan was 1,838 MW (1). All of this capacity is in the Gharo to Keti Bandar and Jhimpir regions of Sindh Province, where wind is driven by the southwest monsoon. The strongest wind speeds are in the summer months of the monsoon season. Mean wind speeds of 7.3 m/s at 80 m are reported (24, 25). Pakistan's demand also peaks in summer. In India, active phases of monsoon circulation are accompanied by increased wind speeds and reduced temperature and cooling demand (26-28). It has been reported that monsoon breaks bring the reverse (26).

1.4 Closest Prior Work

We note that system-specific correlations between resource and demand will likely result in location-specific findings. In a study spanning 39 years and 42 countries, Tong and colleagues found that the most reliable solar and wind systems were wind-heavy, meeting national electricity demand for 72 to 91 percent of hours (29). The balancing area of the Public Service Company of New Mexico showed load correlations of 0.300 with solar and −0.192 with wind (30). Its authors note that, in simulations, more than doubling solar resources barely moved the 8 p.m. net load peak (30). To the best of our knowledge, no peer-reviewed study has investigated the timing of Pakistan's annual peak hour and migration. Ember's report on the peak shifting to the evening is qualitative (3). A study performed for the fiscal year 2020-21 using national data showed two peaks: one around noon, and one at dusk (31). A recent presentation described the duck curve (the midday dip and steep evening rise in grid demand as rooftop solar grows) for the fiscal year 2025 and the potential costs associated with meeting peak demands (32).

1.5 Aims and Hypotheses

This study examines which variable resource meets Pakistan's binding hours, and if cost-minimized planning accounts for it. The binding hours refer to the highest-demand hours in a fiscal year, used as a proxy for the hours when the system is most stretched (Section 2.4). The primary analysis is conducted on the top 50 binding hours. Other analysis is conducted for the 1 hour, 10 hour, and 100 hour binding windows. The metered hourly demand during FY2016 to FY2025 is obtained from the National Power Control Centre (NPCC). The metered hourly generation for FY2024 and FY2025 is obtained by resource category. For each resource, the peak-coincidence ratio is calculated by dividing the mean of the resource's generation over the binding hours by the mean of the resource's annual generation. This is an approximate capacity value comparison (20, 21). It is not a substitute for a complete comparison. Throughout the study, two conditions apply. First, the demand figures are load served plus recorded load management, which may miss unrecorded rationing, and are net of behind-the-meter solar; hence, the evening peaks are considered lower bounds. Second, the figures for wind plants are fully represented in the data, and the same is not true for solar, where only about 680 MW of utility-scale plants are metered.

We test three hypotheses. H1: between FY2016 and FY2025, the binding hours moved from the afternoon into the evening. H2: at the binding hours of FY2025, wind delivers more than its annual average output and utility-scale solar delivers less. H3: when estimated distributed solar output is added back to demand, the binding hours return to the afternoon.

2. METHODS

2.1 Data Sources

The research utilizes three data sets. The principal data set is the NPCC Hourly System Record for FY2016 to FY2025. Pakistani fiscal years are from July to June. This data set provides the hourly system demand for all ten years and the hourly generation for FY2024 and FY2025. The data set for previous years shows generation columns, but the values are zero. Therefore, analysis for this research is limited to generation for FY2024 and FY2025 for wind and solar. The data sets were provided under permission by the Independent System and Market Operator and are to be analyzed and reported in an aggregated form (33).

The secondary data set is composed of 129 Fuel Charges Adjustment (FCA) determinations for the distribution companies of the former Water and Power Development Authority (WAPDA), issued by the National Electric Power Regulatory Authority (NEPRA) from October 2013 to March 2026 (34). Each determination reports the energy purchased from each fuel in GWh, with its share and cost. Eighty-three determinations passed three consistency checks in full: fuel-level GWh summed to the filed total, the shares summed to 100 percent, and the cost per kWh matched the stated rate. A further 35 wind and 35 solar values were recovered from determinations whose tables failed on other rows. Each recovered value passed its own plausibility test: the monthly total implied by its GWh and filed share had to fall within 30

percent of the median total filed for the same calendar month in nearby years. The resulting wind series covers 118 months and is used only as a cross-check (Section 2.7).

According to NEPRA's latest report on the state of the industry, wind capacity is reported at 1,838 MW, with utility-scale solar at 680 MW. Both numbers are the same across the two years studied. Solar capacity was already at 680 MW as of June 30, 2023 (1). Capacity from other renewable energy sources, like distributed solar, is not included in these capacity figures. Distributed solar capacity was estimated between 22.6 and 32.5 GW in a satellite study, and 33.4 GW in a household survey (2). This capacity shows up only as suppressed demand. The capacities assumed for distributed solar in Section 3.7 are drawn from these estimates, as explained there. The satellite estimate carries a margin of ±18.2 percent. Other estimates based on imports put distributed solar capacity at 38 GW or higher (3, 4). These estimates are considered an upper bounding estimate. The CPPA-G's contracted capacity for FY2025 also fell by 9.6% (1), from 42,512 MW to 38,431 MW. This change is from the expiration of contracts primarily on thermal power plants. The effects of the shifting peak demand, which is the focus of this study, are not related to the loss of these contracts.

2.2 What the Demand Series Contains

Computed system demand is reported in the NPCC series. The NPCC operator represents this demand as served system load plus the 'recorded load management' in this series. This identity holds within 0.5 MW on 99.99% of all hours reported in the series for FY2016 to FY2023. Change in the workbook format for FY2024 and FY2025 means demand equals total generation of the system plus load management on 95.4% of hours, with a small positive residual consistent with imports. As the recorded load management may not capture all rationing, such as shedding at the distribution level, series values are considered lower bounds of true system demand. In addition, there is behind the meter solar generation, which further reduces recorded system demand, and is also represented net in this series. In this paper, demand means this recorded quantity. It is net of behind-the-meter solar only, so it is not net load in the usual sense, which also subtracts utility-scale wind and solar.

This series is representative of the ex-WAPDA grid operated by the National Transmission and Despatch Company (NTDC). It should be noted that K-Electric, which is located in the metropolitan areas of Karachi and has its own self-generation and load, is outside the scope of this series. A cross-check of monthly generation against FCA filings (Section 3.5) supports the above representation.

It was only necessary to set a small number of rows to missing. Ten rows of nighttime solar on 1 and 2 February 2025 were set to missing, because they recorded 60 to 171 MW of solar output at night, an error in assigning output to sources. Demand for 29 hours around the January 2021 and January 2023 grid disturbances were set to missing. Demand for 6 rows for FY2018, which were estimated, were retained, and flags were left in place. These hours are not in the top 50 demand hours.

2.3 Timestamp Convention

Gami and others (35) estimate that ambiguity around timestamps by one hour can impact capacity value by up to 41.8%. We therefore tested the convention against the data. We found that in 11 of 12 months, the timestamp of the first non-zero solar generation corresponds to the computed time of sunrise at 31°N, 71°E, which is only possible if the timestamp marks the beginning of the hour. The point 31°N, 71°E is a rounded location near the grid's center; its sunrise times lie within about four minutes of those at the load-weighted centroid used in Section 3.1. Because the workbook format changed between years, the test was repeated for each fiscal year separately. The first non-zero hour matched sunrise in 11 of 12 months in FY2024 and 11 of 12 in FY2025, so both years use the same convention; in the one exception, September, sunrise falls within a minute of 06:00. Sunrise and sunset are computed with the NOAA solar-position equations. All results of the analysis reported in this paper have been repeated and re-analyzed shifting timestamps by −1 and +1 hour (Section 3.6).

2.4 Defining Binding Hours

The fifty binding hours represent the fifty periods of highest computed demand for a given fiscal year. We call them binding because they are the hours in which the system is most likely to run short. They are a proxy. The operator data do not include available generating capacity, so the reserve margin cannot be computed hour by hour, and recorded load management is not a pure measure of shortage, since some of it is applied for commercial reasons (Section 4.5). In Pakistan's Competitive Trading Bilateral Contract Market (CTBCM), the Net Cost of New Entry is set using the fifty critical hours of lowest reserve of the preceding year (36), a related but different set of hours. The nearest analogue to this study uses the fifty periods that represent the net-load peaks of Korea (37). The choice remains unsettled. The windows of binding hours vary from the top ten (35, 38) to the top hundred (39). Munoz and Mills (40), citing earlier work by Madaeni and colleagues, note that a threshold below the top 30 percent of hours can underestimate solar's capacity value. Their own simulations show the opposite risk at high penetration: a capacity-factor approximation over the top load hours, which ignored the shift of the riskiest hours into the evening, overstated solar's capacity value by about 68 percent at 20 percent penetration (40). Recorded demand is already net of behind-the-meter solar, so the binding hours move with that shift. Section 3.6 repeats the main comparison for two other sets of stressed hours: the fifty hours with the most recorded load management, and the fifty hours of highest served load.

2.5 Contribution Metrics

The peak-coincidence ratio is a resource's mean output across the N highest-demand hours divided by its mean output across all hours of the fiscal year:

$$R_N = \frac{\frac{1}{N}\sum_{t \in T_N} P_t}{\frac{1}{|Y|}\sum_{t \in Y} P_t} \qquad \text{(Eq. 1)}$$

where P_t is the resource's output in hour t, T_N is the set of N highest-demand hours, and Y is the set of all hours in the year. The ratio is dimensionless and not influenced by uniform bias in demand. A value greater than 1 means that the resource is able to deliver more than its annual average during the peak hours. We do not propose a new measure. From literature, Madaeni et al. concluded that, among the methods they compared, the best approximation of the effective load carrying capability of a resource is obtained by averaging the capacity factor over peak hours, and reported a root mean square error of 4.12 percentage points of capacity value, compared with 11.9 to 44.4 for the other methods (38). Frew et al. provide an alternate expression for the same concept (39). Capacity factors are reported where the denominator is known. In addition, the Pearson correlation of hourly system demand and hourly resource output is reported for the full year, May to September, and the evening window of 19:00 to 01:00. The May to September window is the headline measure, because full-year correlations mostly reflect demand and wind both being high in summer. Within a July to June fiscal year, May to September joins July to September of one year with May and June of the next, so it spans two different summers. Correlations are therefore also reported for May to September 2024, the one complete calendar season in the generation data. The results are reported as distributions across the 50 binding hours and include minimums and near-zero counts so that no single point is relied upon. The fifty binding hours are not fifty independent observations, since a few hot days can supply many of them. We therefore report how many distinct days and months they cover, counting a day from 06:00 to 06:00 so that a late evening and the small hours after it stay together. Uncertainty ranges are computed by resampling whole days: each replicate draws the days of a fiscal year with replacement, rebuilds the year, selects its fifty highest-demand hours and recomputes the statistic. The ranges are the 2.5th and 97.5th percentiles of 2,000 replicates. The same resampling gives ranges for the correlations, which are more reliable than p-values because neighboring hours are not independent.

2.6 Separating Season from Hour of Day

It is possible that elevated wind output during peak hours represents the seasonal peak of wind, i.e. strong wind during the months of highest system demand. Likewise, it is possible that the diurnal peak of wind occurs during the hour of peak system demand. To test these hypotheses, measurement of wind system output is informative; however, the 2002 to 2005 mast data (25), measured well below modern turbine hub heights, are an imperfect guide, so metered fleet output is used. The top-50 ratio decomposes exactly as

$$R_{50} = S \times D \times K \tag{Eq. 2}$$

with each factor built from the month m(t) and hour of day h(t) of every binding hour t in the set T_{50}:

$$S = \frac{\frac{1}{50} \sum_{t \in T_{50}} \overline{P}_{m(t)}}{\overline{P}_Y} \tag{Eq. 2a}$$

$$D = \frac{\sum_{t \in T_{50}} \widetilde{P}_{m(t),\,h(t)}}{\sum_{t \in T_{50}} \overline{P}_{m(t)}} \qquad \text{(Eq. 2b)}$$

$$K = \frac{\sum_{t \in T_{50}} P_t}{\sum_{t \in T_{50}} \widetilde{P}_{m(t),\,h(t)}} \qquad \text{(Eq. 2c)}$$

Here $\bar{P}_Y$ is the resource's mean output over the year, $\bar{P}_m$ its mean output in month m, and $\tilde{P}_{m,h}$ its mean output at month m and hour h over the hours that are not binding hours. The seasonal factor S measures how strong the resource is in the months of the binding hours. The diurnal factor D measures how strong it is at their hours of day, relative to those months. The day-selection factor K compares output at the binding hours with output at the same months and hours on other days, and so captures whether the high-demand days were windier or sunnier than typical days. Matching each binding hour to its own month and hour keeps K from absorbing differences in timing; with a single reference month and hour, binding hours after dark would lower solar's K instead of its D.

2.7 Cross-Check Against Regulatory Filings

The FCA archive is compiled by a different institution, for billing and at monthly resolution, but it draws on the same underlying metering as the hourly record. It is therefore a cross-check, not independent confirmation. Three comparisons are performed: agreement on basis, i.e. monthly generation by fuel over the 10 overlapping months; monthly wind profiles pooled over twelve years against the hourly data; and year-to-year variation in monsoon winds. Only 10 of the 24 months of FY2024 and FY2025 are compared, because they are the only months in that window whose determinations passed all three consistency checks in Section 2.1. Twelve failed them, mostly because text extraction lost the hydel row or shifted a decimal point, and two (April and July 2024) were not among the 129 determinations collected. The final comparison uses ratios of same-month wind capacity factors in consecutive years, which show how much monsoon wind varies between years. Because these are ratios of capacity factors, growth of the wind fleet over the period does not affect them. Capacity is taken from the year-end levels of the International Renewable Energy Agency (IRENA), using linear interpolation (41). IRENA reports the fleet at 1,845 MW, against 1,838 MW from NEPRA, a 7 MW difference in how the two registries count capacity.

2.8 Robustness Checks

Six sensitivity axes are shown with the headline results: timestamp adjustments by 1 hour in either direction; window size; capacity denominator; other definitions of stressed hours (Section 2.4); an allowance for curtailment of wind; and a behind-the-meter adjustment to estimate gross demand as:

$$G_t = N_t + C \times c_t \qquad \text{(Eq. 3)}$$

where N_t is recorded demand, C is an assumed distributed solar capacity, and c_t is the metered capacity factor of utility-scale solar, used as a proxy for distributed output. This adjustment is kept separate from the headline results because distributed solar capacity is uncertain; the satellite estimate alone carries a margin of plus or minus 18.2 percent (2). Because distributed capacity grew quickly, the adjustment is also run with capacity rising through the period, linearly from C/4 at the start of FY2024 to C/2 at its end and to C at the end of FY2025. This ramp is an assumption, loosely based on panel imports, about two-thirds of which arrived in calendar 2024 and the first half of 2025 (2). Curtailment of wind is not recorded in the data, so its effect is bounded instead (Section 3.6). The wind ratio is recomputed as if all of the gap between the metered annual capacity factor and the 32 to 35 percent reported for the corridor (Section 4.5) were curtailed output outside the binding hours, which is the case least favorable to wind.

3. RESULTS

3.1 The Binding Hour and Its Migration

Every annual peak falls between June and September, so the season of peak demand does not move over the study period. The hour of day does (Table 1).

Table 1. Annual system peak, FY2016 to FY2025.

Fiscal year	Peak date	Peak hour	Peak demand (MW)
2016	25 Jun 2016	13:00	23,287.9
2017	6 Jun 2017	11:00	25,495.6
2018	4 Jun 2018	16:00	26,741.2
2019	2 Aug 2018	15:00	25,627.2
2020	11 Sep 2019	14:00	26,251.6
2021	9 Jun 2021	15:00	28,253.3
2022	28 Jun 2022	15:00	31,271.4
2023	24 Jun 2023	16:00	30,188.8
2024	22 Aug 2023	14:00	30,150.3
2025	20 Jun 2025	23:00	29,201.2

Peaks have been in the 11:00 to 16:00 window for nine years in a row. We observe a peak at 23:00 in FY2025, with no intermediate years to that peak. Demand peaked at 31,271 MW in FY2022, dropping to 30,189 MW in FY2023, 30,150 MW in FY2024 and 29,201 MW in FY2025. Population and connection growth in this time means demand should have increased, and this decline is all the more notable. We can see the migration more reliably in the fifty binding hours (Table 2).

Table 2. Evening share of the fifty binding hours, with evening defined as the fixed window 19:00 to 00:59 PKT, its 95 percent range from resampling whole days, and the number of distinct days and months on which the fifty hours fall (days run from 06:00 to 06:00).

Fiscal year	Evening share (%)	95% range	Distinct days	Months
2016	12	2 to 28	16	2
2017	2	0 to 8	11	3
2018	4	0 to 12	14	3
2019	2	0 to 10	21	4
2020	14	0 to 28	18	4
2021	6	0 to 18	13	3
2022	18	6 to 30	9	1
2023	24	10 to 40	9	2
2024	32	14 to 40	12	2
2025	90	80 to 98	17	2

Between FY2016 and FY2021, the evening share ranged between 2 and 14 percent, showing no definite pattern. In FY2022, it rose to 18 percent, and continued rising to 24, 32 and finally 90 percent. The net change of 58 percentage points between FY2024 and FY2025 was almost three times the total change between FY2016 and FY2024. The evening window is fixed at the hour labels 19 to 23 and 0. An analysis of the modeled sunset of the load-weighted demand centroid (29.376°N 70.953°E) showed that the fixed window differed by one hour or less in each year, with 46 hours after sunset against 45 in the window in FY2025. Therefore, the result is insensitive to the definition. The fifty binding hours of FY2025 fell on 17 distinct days in 2 months, against 12 days in 2 months in FY2024. Resampling whole days, the FY2025 evening share has a 95 percent range of 80 to 98 percent, and FY2024's 14 to 40 percent. For more information, see Table 3 and Figure 1.

Table 3. Binding hours by time-of-day bucket.

Fiscal year	00-05	06-11	12-17	18-23
2016	0	9	35	6
2017	0	7	40	3
2018	0	8	40	2
2019	0	0	49	1
2020	0	0	42	8

Fiscal year	00-05	06-11	12-17	18-23
2021	0	1	46	3
2022	0	4	35	11
2023	2	6	32	10
2024	0	1	33	16
2025	9	0	3	38

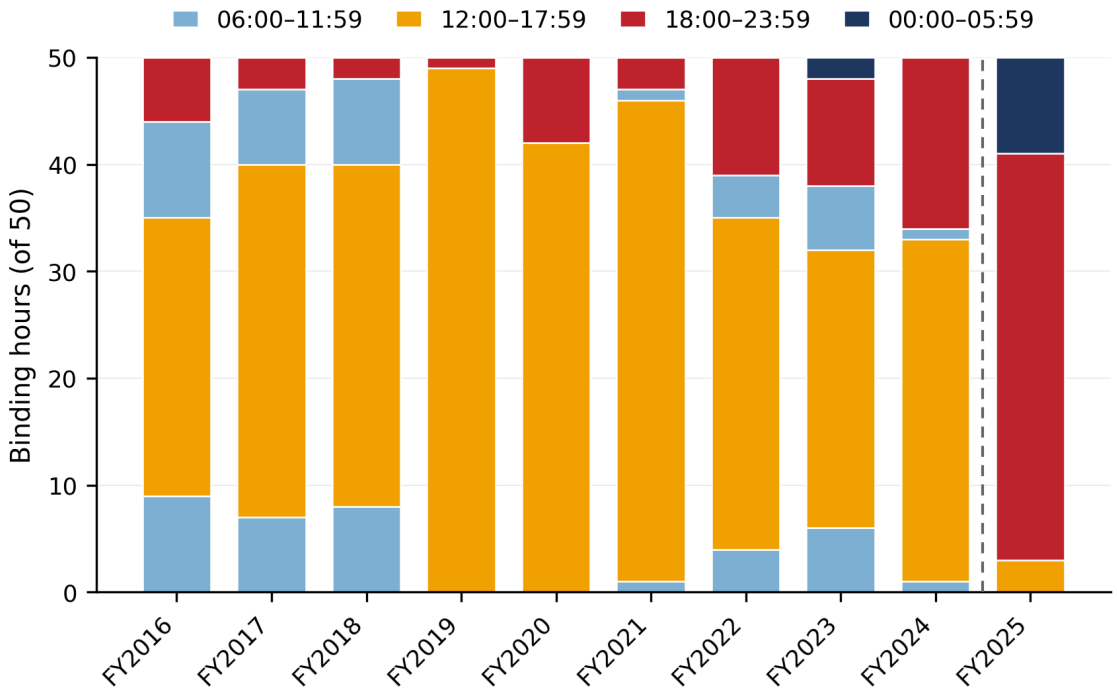


Figure 1. Distribution of the fifty binding hours of each fiscal year across time-of-day buckets, FY2016 to FY2025, stacked chronologically from 06:00 at the base. The dashed line marks the FY2024 to FY2025 transition.

In FY2025, compared to FY2024, binding hours in the afternoon declined from 33 to 3, and compared to FY2019, from 49 to 3. Also, compared to FY2024, the number of binding hours from midnight to 06:00 increased from zero to nine, a bucket empty in eight of the ten years. From FY2024 to FY2025, the binding hours lost almost all of their daylight hours. Load management at the FY2025 peak hour was 4,502 MW, or 15.4 percent of the computed demand. Across the binding hours it averaged 16.3 percent, ranging from 13.9 to 19.0 percent. The corresponding numbers for FY2024 were 5,507 MW, 18.3 percent, a binding-hour average of 18.9 percent, and a range of 12.9 percent to 22.2 percent. This load

management is added back into the figures, but unrecorded rationing is not; therefore, every peak reported is a lower bound.

Figure 2 shows mean demand at each hour of the day over May to September of each fiscal year. Between FY2024 and FY2025, mean demand at 14:00 fell by 2,241 MW and mean demand at 23:00 rose by 210 MW. The binding hours therefore moved mainly because the afternoon peak was shaved, not because evening demand grew, which also fits the fall in the annual peak since FY2022.

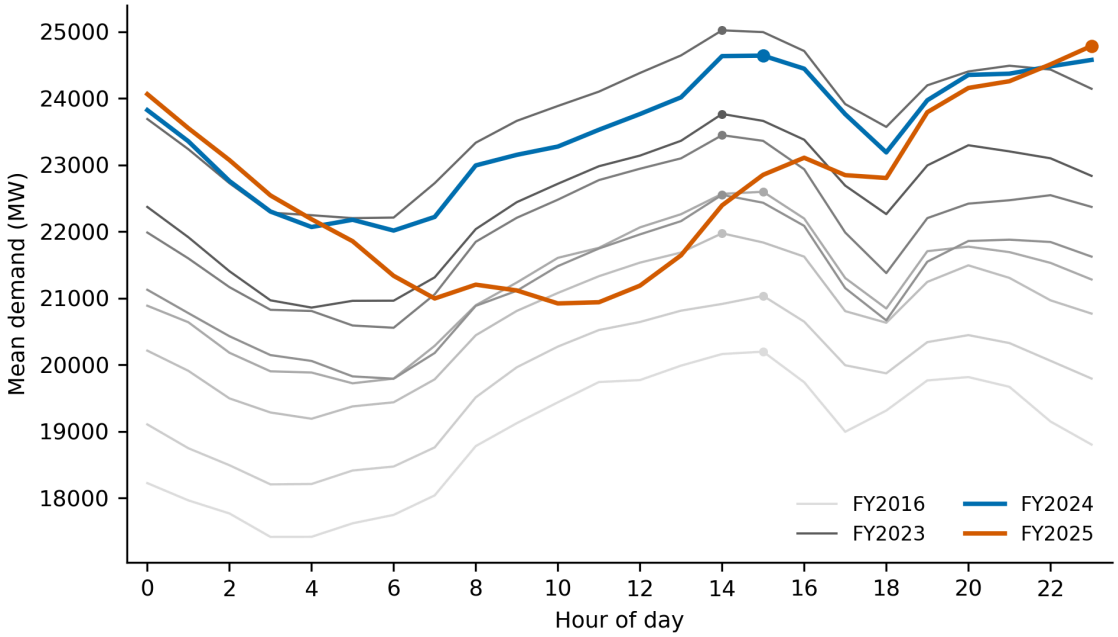


Figure 2. Mean computed demand by hour of day over the May to September hours of each fiscal year, FY2016 to FY2025. Grey lines run from FY2016 (lightest) to FY2023 (darkest); FY2024 is blue and FY2025 orange; dots mark each year's highest hour.

3.2 Resource Delivery at the Binding Hours

Table 4 gives the peak-coincidence ratio (Eq. 1) for each resource, fiscal year and window.

Table 4. Peak-coincidence ratios by resource, fiscal year and window. The last column gives the 95 percent range of the top-50 ratio from resampling whole days.

Resource	Fiscal year	Top 1	Top 10	Top 50	Top 100	Top-50 95% range
Wind	2024	3.248	2.809	2.717	2.719	2.457 to 3.017
Wind	2025	2.073	2.031	2.108	1.952	1.768 to 2.422

Resource	Fiscal year	Top 1	Top 10	Top 50	Top 100	Top-50 95% range
Solar	2024	2.442	1.533	1.310	1.363	1.088 to 1.703
Solar	2025	0.000	0.000	0.124	0.205	0.000 to 0.338

Wind exceeds unity at every window in both years, ranging from 1.952 to 3.248. Solar exceeds unity at every window in FY2024 and at none in FY2025, where it ranges from zero to 0.205. Wind's ratio exceeds solar's in all eight paired comparisons. The resampled ranges for wind and solar do not overlap in either year. Table 5 gives the underlying quantities.

Table 5. Mean output at the fifty binding hours against annual mean output, with capacity factors on the State of Industry Report denominators (n = 50 hours).

Resource	Fiscal year	Top-50 mean (MW)	Annual mean (MW)	Annual CF	Top-50 CF	Denominator (MW)
Wind	2024	1,218.6	448.5	0.244	0.663	1,838
Wind	2025	926.0	439.4	0.239	0.504	1,838
Solar	2024	144.3	110.2	0.162	0.212	680
Solar	2025	16.2	130.0	0.191	0.024	680

Wind's capacity factor is about 0.24 for the year overall, 0.663 at the binding hours in FY2024, and 0.504 in FY2025. Solar's annual capacity factor increases from 0.162 to 0.191 in the 2-year period, and its binding-hour capacity factor decreases from 0.212 to 0.024. The rise in solar's annual capacity factor, with reported capacity unchanged at 680 MW, is large for a year-to-year change in weather (Section 4.5). The 680 MW includes three 50 MW plants at Sukkur. NEPRA lists them from June 2023 (1), but Renewables First reports that they were commissioned in February 2024 (4), so they produced for all of FY2025 and only part of FY2024. The rise most likely reflects more of the listed fleet producing. The peak-coincidence ratio needs no capacity figure, and in FY2025, the headline year, the whole fleet ran all year, so that year's comparison does not depend on this. Given that means alone are misleading, complete information is in Table 6 and Figure 3.

Table 6. Distribution of output across the fifty binding hours. Near-zero is defined as below 10 percent of nameplate, that is 183.8 MW for wind and 68 MW for solar.

Resource	Fiscal year	Min (MW)	P25	Median	P75	Max (MW)	Hours near zero
Wind	2024	798	1,081.8	1,217.0	1,362.8	1,650	0
Wind	2025	0	721.2	917.5	1,147.8	1,458	1

Resource	Fiscal year	Min (MW)	P25	Median	P75	Max (MW)	Hours near zero
Solar	2024	0	0.0	147.5	242.0	350	16
Solar	2025	0	0.0	0.0	0.0	360	47

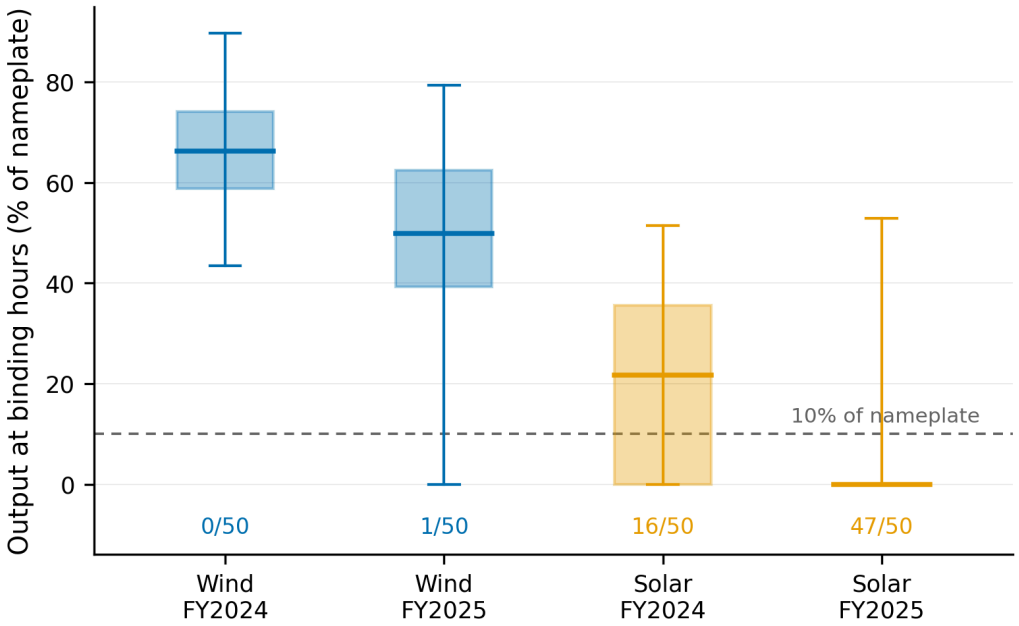


Figure 3. Output across the fifty binding hours as a percentage of nameplate (1,838 MW wind, 680 MW solar). Boxes show the interquartile range and median, whiskers the minimum and maximum. The dashed line marks the 10 percent near-zero threshold, and counts below each box give the hours at or below it.

Wind's lowest FY2024 binding hour generates 798 MW, equal to 43% of its nameplate. Wind's FY2025 distribution is wider. It has an hour of zero generation, discussed with curtailment in Section 3.6. Therefore, in 49 of 50 hours wind generates above the near-zero level. Solar's ratio for FY2024 is also greater than 1, but the first quartile is still zero. Therefore, solar produced near-zero output for about a third of the binding hours. For FY2025 solar's median, and both quartiles are zero. Near-zero output is also the case for 47 of the 50 hours of the period. The remaining three hours produced almost all of the 16.2 MW mean. In all ten of the highest-demand hours of FY2025, solar's output was exactly zero. The FY2024 top 10 hours had a mean of 168.9 MW. All ten of the highest-demand hours for FY2025 occurred after sunset. That utility solar produces nothing at those hours follows from the position of the sun and needs no data to establish. What the data add is that the binding hours moved to that time, and how much wind delivers at them.

3.3 Correlation Between Output and Demand

Table 7 gives Pearson correlations between hourly output and hourly demand.

Table 7. Pearson correlations between hourly resource output and hourly computed demand. Missing values are handled by pairwise deletion, so only the ten artifact rows in FY2025 solar reduce n below the full-year count. The 95 percent ranges come from resampling whole days. The last two rows use May to September 2024, which spans the end of FY2024 and the start of FY2025.

Resource	Fiscal year	Window	r	p	n	95% range
Wind	2024	Full year	+0.697	<0.001	8,784	0.651 to 0.735
Wind	2024	May-Sep	+0.505	<0.001	3,672	0.426 to 0.580
Wind	2024	Evening	+0.705	<0.001	2,196	0.655 to 0.749
Wind	2025	Full year	+0.483	<0.001	8,760	0.422 to 0.538
Wind	2025	May-Sep	+0.317	<0.001	3,672	0.220 to 0.410
Wind	2025	Evening	+0.510	<0.001	2,190	0.440 to 0.575
Solar	2024	Full year	+0.116	<0.001	8,784	0.092 to 0.140
Solar	2024	May-Sep	−0.036	0.028	3,672	−0.075 to 0.005
Solar	2024	Evening	undefined	n/a	2,196	n/a
Solar	2025	Full year	−0.086	<0.001	8,750	−0.112 to −0.060
Solar	2025	May-Sep	−0.347	<0.001	3,672	−0.403 to −0.294
Solar	2025	Evening	+0.018	0.401	2,180	n/a
Wind	2024/25	May-Sep 2024	+0.309	<0.001	3,672	0.209 to 0.408
Solar	2024/25	May-Sep 2024	−0.141	<0.001	3,672	−0.186 to −0.100

Within the May to September season, wind correlates positively with demand in both years (+0.505 and +0.317) and solar negatively (−0.036 and −0.347). Over the single calendar season of May to September 2024, the correlations are +0.309 for wind and −0.141 for solar. Wind correlates positively in all six fiscal-year cells considered, and best in the evening window, which contains the binding hours, at +0.705 and +0.510. Solar is marginally positive to negative over the years, with the most negative value in the FY2025 peak season at −0.347. Solar had zero recorded output in the FY2024 evening window, thus the coefficient is undefined. In FY2025 the only nonzero evening value is a single −0.2 MW reading; FY2024 records solar in whole megawatts, while FY2025 records unrounded values, including small negative readings. The value in the FY2025 evening window is +0.018 ($p = 0.401$), which therefore carries no information. The FY2024 May to September value ($p = 0.028$) is significant only at the 0.05 level, though

its resampled range includes zero. Because neighboring hours are not independent, all these p-values are overstated; the day-resampled ranges in Table 7 do not share this problem. The balancing area of New Mexico showed positive correlation of solar with load at +0.300, and negative correlation of wind with load at −0.192 (30), the reverse of the ordering here. That study covered one balancing area and simulated its solar series from 2013 irradiance. In this study, both the wind and solar series are metered.

3.4 Season Against Hour of Day

Table 8 applies the decomposition in Eq. 2, with each binding hour matched to its own month and hour of day (Eq. 2a to 2c).

Table 8. Three-factor decomposition of the top-50 ratio, matched to the month and hour of each binding hour. The product of the three factors equals the top-50 ratio. The range for K comes from resampling whole days.

Resource	FY	Seasonal (S)	Diurnal (D)	Day-selection (K)	K 95% range	Product	Ratio
Wind	2024	2.138	1.036	1.226	1.041 to 1.450	2.717	2.717
Wind	2025	1.492	0.968	1.459	1.138 to 1.774	2.108	2.108
Solar	2024	0.932	1.393	1.009	0.913 to 1.110	1.310	1.310
Solar	2025	1.089	0.105	1.086	0.883 to 1.215	0.124	0.124

For wind, the seasonal factor is 2.138 in FY2024 and 1.492 in FY2025, the diurnal factor 1.036 and 0.968, and the day-selection factor 1.226 (95 percent range 1.041 to 1.450) and 1.459 (range 1.138 to 1.774). In FY2024 the seasonal factor carries most of the ratio. In FY2025 the seasonal and day-selection factors are about equal, and the day-selection range lies above 1 in both years. A diurnal factor close to 1 means wind at the binding hours of day was close to its average for those months, so wind's advantage does not depend on the hour of day. In June to August, mean wind output at 23:00 was 80 percent of its output at 16:00 in FY2024 and 78 percent in FY2025. The metered output agrees with the 2002 to 2005 mast data, which showed wind strongest in the afternoon and weaker in the late evening (25).

Insufficient solar resource during the FY2025 binding period is explained by the binding hours occurring during the night. For solar, the diurnal factor carries the result: 1.393 in FY2024, when most binding hours fell in daylight, and 0.105 in FY2025, when almost none did. Matching each binding hour to its own month and hour places the effect of the 16 FY2024 evening binding hours in the diurnal factor; with a single reference hour, those hours had pulled the day-selection factor down instead. Solar's day-selection factor is 1.009 in FY2024 and 1.086 in FY2025. Both ranges include 1, so the data do not show whether the high-demand days were sunnier or cloudier than typical days.

3.5 Cross-Check Against Regulatory Filings

Table 9 compares monthly generation by category in the two sources over their ten overlapping months.

Table 9. Basis agreement (NPCC divided by FCA) between NPCC hourly generation and NEPRA FCA filings, ten overlapping months.

Category	Mean ratio	CV (%)	Min	Max
Hydel	1.009	0.24	1.005	1.013
Nuclear	1.004	0.09	1.002	1.005
Wind	1.000	0.27	0.996	1.003
Thermal (lumped)	1.000	0.14	0.998	1.003
Solar	0.941	5.08	0.806	0.965
Bagasse	1.520	26.50	0.993	2.143
Total	1.002	0.19	0.998	1.005

This study's major assertions rest on close agreement. Wind agreement is within 0.4 percent in the worst month, and has a coefficient of variation of 0.27 percent, and the system total agrees at 1.002. Agreements among thermal, hydel and nuclear are of the same order. Solar agrees at 0.941. Solar FCA filings indicate about 6 percent more than the NPCC data, and is most likely due to the difference in the definition of grid connected solar. Bagasse, at 1.520, is not usable. The variations do not impact the conclusion regarding wind. The 6 percent gap for solar is not material when considering solar binding hour capacity factor fell about ninefold between the two years. Hence, basis agreement is supported for wind, thermal, hydel, nuclear and total, but not for bagasse and solar.

Wind shape for FY2024 and FY2025 has a correlation of $r = 0.901$ and $r = 0.819$ respectively, with respect to 12 year pooled monthly wind data. The mean of the two years has a correlation of 0.929 with the pooled data ($n = 12$, $p \leq 0.001$; Spearman's correlation of 0.909 and 0.853 for FY2024 and FY2025 respectively, 0.986 for the mean). Thus wind shape for 2 years replicates long term seasonal variation. Monthly monsoon wind output of a given year is expected to vary by a quarter to a third in adjacent years (interquartile range 0.746 to 1.329 across 36 May to September pairs: 9 in May, 8 in June, 5 in July, 7 in August and 7 in September; the clean months alone give 19 pairs). The ratio of wind output for August 2024 (FY2025) to August 2023 (FY2024) is 0.495. Among 7 August pairs, it was the lowest, and among 36 pairs, it was the third lowest. Part of the fall in wind's ratio from 2.717 to 2.108 in the two years, can be attributed to the normal interannual variation in wind resources. The result for both years indicates the same direction, however the difference in value is only valid for the years under consideration.

3.6 Robustness

No conclusion changes when timestamps are shifted by one hour in either direction. The largest change observed in absolute terms is the decrease in the FY2025 evening share from 90% to 76% under the +1 hour adjustment. The remaining headline figures changed by at most 0.02 in absolute terms. The evening share is above 75% with both adjustments.

Changing the allowed window size does not change the relative ordering of wind and solar (Table 4, Figure 4). Munoz and Mills (40) note that narrow windows can understate solar. Consistent with this, wider windows admit more daytime hours, and in FY2025, solar's ratio rose from zero to 0.205 at the top hundred, much less than wind's ratio at 1.952. In FY2024, solar ratio was 2.442 for the top-1 window, which was higher than its top-50 ratio, because that year's single peak hour occurred in the afternoon.

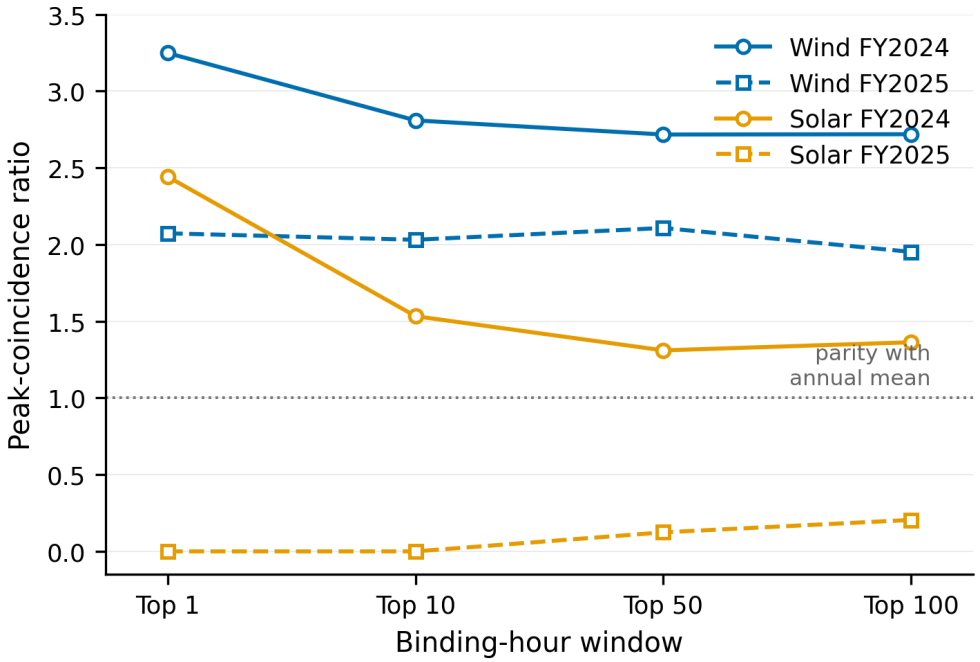


Figure 4. Peak-coincidence ratio (Eq. 1) by binding-hour window for both resources in both fiscal years. The dotted line marks parity with the annual mean.

Recomputing FY2025 wind's top-50 capacity factor on IRENA's 1,845 MW instead of 1,838 MW gives 0.502 against 0.504, so the registry gap drives no result. The analysis rests on 8,743 to 8,784 hours per fiscal year, with 8,750 for FY2025 solar after removal of the ten artifact rows, and none of the flagged or removed hours falls in any top-fifty window.

For the fifty hours with the most recorded load management, wind's ratio is 0.864 in FY2024 and 0.616 in FY2025, and solar's 0.529 and 0.999. For the fifty hours of highest served load, which is computed demand less recorded load management, wind's ratio is 2.543 and 2.046, and solar's 0.632 and 0.000.

Wind's ratio exceeds solar's in every case except the load-management definition in FY2025, where both fall below 1. The evening share of the fifty highest served-load hours is 64 percent in FY2024 and 86 percent in FY2025, so the move to the evening depends partly on how load management is recorded. The hours of lowest reserve used by the market rules (36) cannot be identified, because the data do not include available capacity.

The operator data do not record when wind was curtailed, so metered output may understate the wind resource. If wind were held back mainly when demand was low, the annual mean would be understated and the peak-coincidence ratio overstated. A bound needs no curtailment data. Suppose the whole gap between the metered annual capacity factor and the 32 to 35 percent reported for the corridor (Section 4.5) were curtailed output, all of it outside the binding hours, which is the case least favorable to wind. The FY2025 top-50 ratio would then fall from 2.108 to between 1.44 and 1.57, and the FY2024 ratio from 2.717 to between 1.89 and 2.07. Both stay well above 1 and above solar's ratio in each year (1.310 and 0.124). The ratio could fall below 1 only if the uncurtailed annual capacity factor exceeded the binding-hour capacity factor, 0.504 in FY2025 and 0.663 in FY2024, which is above any figure reported for the corridor. The binding-hour capacity factors record what wind actually delivered and are not affected by curtailment at other hours.

Curtailment at low demand could still add to the positive correlation between wind and demand. Restricted to hours with demand above each year's median, wind's correlation with demand is +0.555 in FY2024 and +0.253 in FY2025. The one FY2025 binding hour with zero wind output fell at 23:00 on 20 July 2024. Output declined over several hours, from 302 MW at 18:00 to zero, consistent with calm weather.

3.7 Reconstructed Gross Demand

All values in this section are estimates and are not used in any calculation above. Reconstruction of gross demand is done using Equation 3. The utility-solar profile is used to approximate the distributed solar energy, despite differences in solar orientation and siting. The capacity values are uncertain; the satellite estimate alone carries a margin of ±18.2 percent (2). There are three values that fall in the plausible range (Table 10, Figure 5). The lower value is 5 GW, a deliberately low case covering only grid-connected ex-WAPDA capacity, set just below the roughly 6 GW of net-metered capacity reported nationally (2). The upper value is 25 GW, roughly the grid-connected distributed capacity in the household survey: about 6 GW of net-metered systems and 19 GW of systems behind the meter without net metering (2). The survey's further 8 GW of off-grid systems is left out, because those systems do not draw on the grid. Applied to the ex-WAPDA series, which excludes K-Electric, 25 GW is an upper bound. The central value is 15 GW. It sits below the survey's grid-connected total because rooftop systems typically produce less per kilowatt than utility plants, owing to orientation, shading and dust, and because some systems may power new load instead of replacing grid supply. The cloudy-day test implies about 1.8 GW, a lower bound.

Table 10. Binding hours and resource metrics under reconstructed gross demand.

FY	Assumed BTM	Evening share	Modal hour	Wind top-50 ratio	Solar top-50 ratio	Wind r (full year)	Solar r (full year)
2024	5 GW	0.0%	14:00	2.758	2.572	+0.673	+0.328
2024	15 GW	0.0%	11:00	2.575	3.242	+0.569	+0.629
2024	25 GW	0.0%	12:00	2.256	3.897	+0.465	+0.786
2025	5 GW	10.0%	13:00	2.111	2.581	+0.461	+0.199
2025	15 GW	0.0%	12:00	1.812	3.284	+0.346	+0.617
2025	25 GW	0.0%	10:00	1.786	3.432	+0.242	+0.806

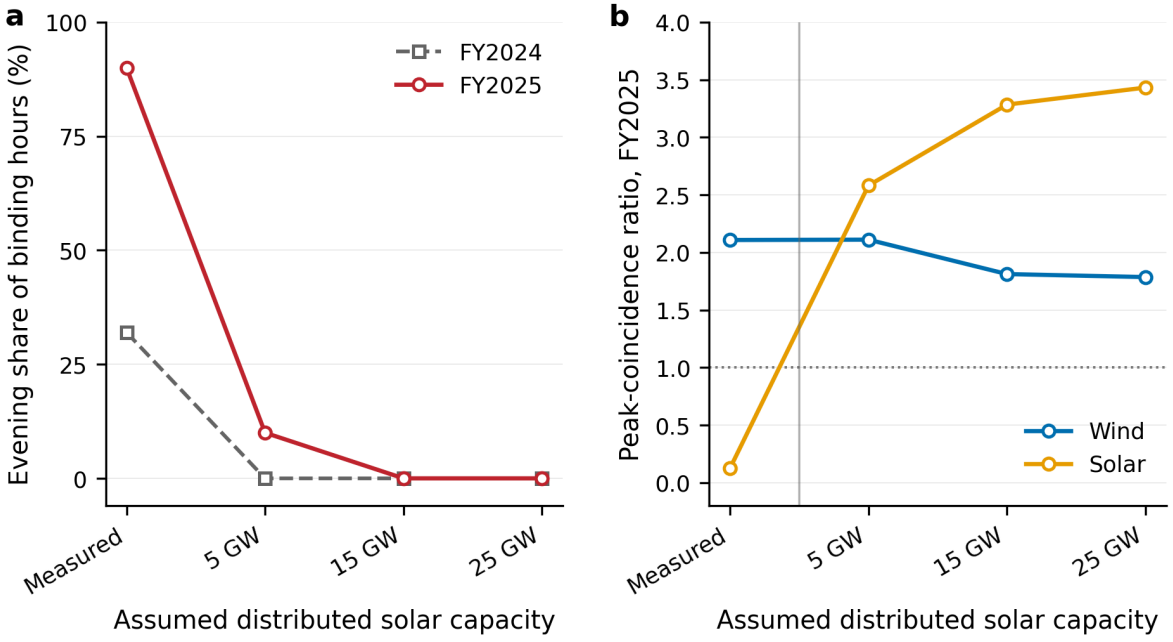


Figure 5. Binding hours and resource delivery under reconstructed gross demand (Eq. 3) at three assumed distributed capacities; all reconstructed values are estimated. (a) Evening share of the binding hours. (b) FY2025 peak-coincidence ratios, with the vertical rule separating measured from reconstructed values.

With capacity held constant, binding hours shift to the afternoons at all levels and in both years, with the evening share in FY2024 falling to zero, and in FY2025 to 10% at 5 GW and zero at 15 and 25 GW. In both years, the most common binding hour falls between 10:00 and 14:00. Removing distributed solar shifts the peak back to the afternoons, as expected if distributed solar moved it. This is partly built in, because adding a solar-shaped term to demand pulls the peak toward midday and raises solar's correlation

by construction, so the reconstruction shows what the system would look like at each assumed capacity, not independent proof.

Positive correlations of wind with demand remain at all levels, from 0.242 to 0.673. Wind's ratios stay above 1, from 1.786 to 2.758. Solar's ratios range from 2.572 to 3.897, and are above wind's ratios at 15 and 25 GW in both years and at 5 GW in FY2025. Solar's correlation with demand for the period May to September is 0.913 at 25 GW in FY2025, against −0.347 as measured.

At most levels considered, solar is the better-matched resource with system demand in the absence of distributed solar.

With capacity ramped through the period as described in Section 2.8, the evening shares at the 15 GW end value are 0 percent in both years and solar's top-50 ratios are 2.568 and 2.956, so the conclusion holds at 15 GW. At 5 GW, however, the FY2025 binding hours stay mostly in the evening (60 percent). Two features of rooftop systems are captured by neither version. Rooftop panels face many directions, unlike the utility plants whose output is used as the proxy, and some rooftop systems now have batteries that move part of their output into the evening. Battery discharge also hides evening demand from the operator, so the reconstruction may overstate how far the peak returns to the afternoon.

3.8 A Test Without Reconstruction

Because the reconstruction is partly circular, the distributed-solar explanation was also tested directly. Utility solar output measures how sunny each day was. If distributed solar suppresses daytime demand, midday demand should rise on cloudy days relative to the same day's evening demand, which tracks the day's cooling load. For each day of FY2024 and FY2025, mean demand from 11:00 to 13:59 was regressed on the mean capacity factor of utility solar over the same hours, with the day's mean demand from 20:00 to 23:59 as a control and a separate intercept for each month. Each rise of 0.1 in the midday capacity factor lowered midday demand by 180 MW (95 percent range 72 to 269 MW, resampling whole weeks), equivalent to about 1.8 GW of distributed solar behaving like the utility fleet. Without the evening control, the effect is 33 MW. This supports the explanation in direction, though the implied capacity is a lower bound. The test is conservative. Cloudy days are also cooler, which lowers demand, and the utility plants sit in a few places, so their output is a noisy measure of sunshine across the grid. Both effects push the estimate toward zero.

4. DISCUSSION

4.1 What the Two Demand Series Show

The measured results for wind and solar at the binding hours show how the wind and solar systems performed with respect to the demand condition they faced. Wind delivered 2.108 times its annual average, and solar 0.124 times its annual average, at the FY2025 binding hours. Section 3.7 shows that in the absence of distributed solar, with capacity held constant, solar would deliver between 2.581 and 3.432 times its annual average at the binding hours, and the binding hours would return to the early afternoon.

The results shown in sections 3.2 and 3.7 point in opposite directions. Section 3.2 shows the performance of solar with respect to Pakistani demand is weak, while Section 3.7 shows it is strong. If distributed solar moved the peak, utility-scale solar's poor measured performance is a result of solar's own success. This cannot be proven with these data, since distributed capacity is estimated, the reconstruction is partly built in, and there is no counterfactual system to observe.

Distributed solar is not the only change that could move the peak. Tariffs rose steeply over the period (2), which encouraged solar adoption but could also have changed when households and businesses use power. Industrial demand, which is concentrated in daytime hours, may have fallen. Hotter nights would raise late-evening cooling demand, and a change in how load management is recorded could shift computed demand between hours. These data cannot separate all of these causes, but two checks bear on them. The move to the evening also appears in served load (64 percent in FY2024 and 86 percent in FY2025), so it is not produced only by the way load management is recorded. Midday demand rises on cloudy days, which distributed solar predicts and the other explanations do not. We therefore describe distributed solar as the most likely cause, not a proven one.

4.2 Why Cost-Minimizing Planning Failed to See This

Planning models reviewed in Section 1.1 place solar above wind, and their cost estimates do not raise questions. These models do not account for delivery at the binding hours, and the reason for this is inherent in the structure of the models. A cost-minimizing model that accounts for an annual energy balance and a reserve-margin constraint will not capture the timing of energy delivery with respect to the timing of scarcity. The LEAP capacity credit is an availability ratio borrowed from other systems (8). The annual wind capacity factor of about 0.24 is the factor that is relevant for levelized cost of energy and wind fares poorly with respect to this. The capacity factor of about 0.504 at the binding hours, which is relevant for adequacy, is not accounted for in any of the Pakistani studies we reviewed.

The devaluation of solar at peak hours is well recognized. Hirth (42) reports the market value of solar in Europe decreasing to low levels at about 15% penetration, with wind values attaining comparable levels only near 30% penetration. This is due to the fact that solar generates in hours in which earlier solar units have already depressed the market. The studies by Brown and Reichenberg (43), the marginal capacity credit study of Korea (37), and the National Renewable Energy Laboratory (44), confirm similar findings. Mills and Wiser (45) report that the capacity part of value erodes first. Munoz and Mills (40) expect that the solar energy capacity will displace the net-load peak into hours solar cannot serve. As opposed to other countries where similar events occur, the changes in Pakistan occur quickly. The evening share of the binding hours in Pakistan rose from 32% to 90% in one year. In other cases, the resource that is being eroded is also the resource that is displacing the peak. In Pakistan, this appears not to be the case. If distributed solar displaced the peak, the displacing fleet, estimated at 22.6 to 33.4 GW (2) or 38 GW or more (3, 4), is far larger than the utility fleet of about 0.68 GW (1) on which the fall is measured, and which could not have moved the peak on its own.

4.3 The Storage Objection

The clear response to energy generated at the wrong time is storage itself. Mitigating the effects of declining value of variable renewable energy sources requires diversity, storage and demand response (46). In a least-cost model, Sadiqa and others (6) find that batteries supply 99 percent of storage by 2050, mostly to move daytime solar output into the evening and night. Without batteries, solar will not be able to shift to the evenings on its own. In one New Mexico balancing area, Lave and Ellis (30) showed that more than doubling solar capacity barely moved the net load peak at 8 pm. Hence, storage is critical and must be considered separately. How much storage is required to make Pakistani solar be equivalent to wind at binding hours is indeterminable from the current data, and is left for future work.

4.4 What Generalizes and What Does Not

Wind's advantage has little hour-of-day component, with diurnal factors of 1.036 and 0.968. Pakistani winds are fastest with the south-west monsoon (June-July), which coincides with peak grid conditions. In FY2024 the advantage was mostly seasonal. In both years the high-demand days were also windier than typical days at the same month and hour, more so in FY2025, though the range is wide. Indian data indicates the seasonal component is also correlated to the monsoon (26). Our Pakistani data show a positive correlation between demand and wind within the May to September season in both years, although Indian monsoon breaks bring high demand and weak wind together (26). Dunning and others (26) note the demand/wind coupling during the Indian monsoon, and Gulagi and others (47) report that 62 percent of Indian wind generation falls in the monsoon. We expect that systems that have wind conditions correlated to monsoon demands would also show the seasonal component to wind output, and systems that do not (like New Mexico (30)) would not.

4.5 Limitations

The two-year window on the data reflects an uneven constraint on the two resources. Solar capacity factors tend to be fairly consistent from year to year, while wind capacity factors can be somewhat more variable (48). For this reason, the applicability of the 12-year FCA to wind is justified. Madaeni and colleagues (38) suggest that the uncertainty in a two-year estimate of capacity value is approximately 6.6 percentage points compared to an 8-year estimate. Wind's output at the binding hours is not guaranteed. The wind fleet showed zero output for one of the binding hours. Accreditation should be granted considering that hour of wind fleet output was zero, and that hour should not be averaged away. Wind capacity factors for both years were well below the 32-35% wind capacity factors reported by the Institute for Strategic Studies, Research, and Analysis (49). While we were unable to obtain the primary research reports, we use our metered values throughout.

Curtailment may explain part of this gap. Wind producers have complained of curtailment since November 2022; the system operator has linked it to the merit order of dispatch and to the distance between the southern wind farms and northern demand (50), and in 2026 an industry body blamed transmission congestion in the Gharo and Jhimpir corridors (51). Neither source gives the energy lost and the hourly data do not record it, so Section 3.6 bounds its effect instead of measuring it. Wind's value also

depends on transmission. The whole fleet sits in Sindh, far from the northern load centers, so congestion on the south-to-north corridor could limit how much additional wind reaches load at the binding hours.

The solar results cover about 680 MW of utility plants, against a distributed fleet thirty or more times larger that is not metered in this dataset. Estimates in Section 3.7 rely on a proxy profile and on uncertain capacity figures, with the satellite estimate alone carrying a margin of ±18.2 percent, and the 25 GW value should be considered an upper bound.

The binding hours are defined by computed demand, which adds recorded load management back to served load, and not all load management reflects a lack of supply. The regulator has penalized distribution companies, four of them ex-WAPDA companies, for load shedding in 2022 that was based on feeder losses (52). Hours with heavy load management may therefore overstate how stretched the system was, which is why Section 3.6 repeats the comparison for other definitions of stressed hours. At the fifty hours with the most recorded load management, neither resource reaches its annual average, which may reflect that much of this shedding follows feeder losses rather than a lack of supply.

The hourly data provided by the operator end in June 2025, so we cannot yet say whether the evening peak persisted in FY2026.

Finally, load management averaged 16.3% at the FY2025 binding hours and 18.9% at the FY2024 binding hours. It is added back into demand, but unrecorded rationing and behind-the-meter solar are not, so the real unconstrained peak during these periods is likely higher than every figure reported.

4.6 Implications

It should be noted that if the binding hour of a system can move by nine hours within a year, adequacy assessments cannot rely on either annual energy or installed capacity alone. Methods employed by the Pakistan market design already set the Net Cost of New Entry using the critical fifty hours of the lowest reserve (36), which are not identical to the highest-demand hours used here, and applying the same reasoning to capacity planning would need no new method. In addition, evaluating peak-coincidence ratios would be a low cost exercise. Each power system operator can determine this value by simply analyzing hourly demand and generation by various resources. If the binding hour partly reflects the deployment of distributed solar, as our results suggest, planning that treats the demand curve as fixed will keep lagging behind it.

5. CONCLUSION

In a single year, the binding hour for Pakistan shifted from the afternoon to late evening. At those hours, wind provided about twice its annual average, and the grid-connected solar provided next to nothing, and a generous allowance for curtailment does not change this. It is worth noting that wind's advantage comes mainly from the monsoon season, not the hour of day, which also exposes it to the monsoon's variability, and consequently, other monsoon regions with summer peak grid conditions may yield similar results. In both years, and especially in FY2025, the high-demand days were also unusually windy. The binding hour

shows solar's collapse, but this does not mean solar is poorly suited to Pakistan, since against demand reconstructed without distributed solar, solar is the better-matched resource. The models that incorporate solar to satisfy the electricity demand are correct from an economic perspective; however, from an adequacy perspective, they miss that solar is misaligned with the binding hours while wind mostly is not. Applying the existing 50 critical hours reasoning to capacity planning would let planning follow the binding hour.

DATA AVAILABILITY

The hourly data for the power systems were provided by the Independent System and Market Operator under permission and cannot be redistributed. The data are available from the operator on request (33). Fuel Charges Adjustments were made public by NEPRA (34).

CODE AVAILABILITY

The analysis code is available from the authors on request.

AUTHOR CONTRIBUTIONS

Both authors designed the study, analyzed the data and wrote the manuscript, and both approved the final version.

ACKNOWLEDGEMENTS

We thank the Independent System and Market Operator for providing the hourly data.

ABOUT THE AUTHORS

Sheraz Hassan is a Grade 12 student at The City School, Lahore, Pakistan. He is interested in using data to study energy systems and public infrastructure. Muhammad Sami Shahid is a Grade 11 student at Trinity School, Lahore, Pakistan, and a research intern at PhysLab, LUMS. He is interested in electrical engineering and physics.

REFERENCES

1. National Electric Power Regulatory Authority. (2026). State of industry report 2025. NEPRA. https://www.nepra.org.pk/publications/State%20of%20Industry%20Reports/State%20of%20Industry%20Report%202025.pdf
2. TransitionZero. (2025). Shedding light on Pakistan's distributed solar revolution. https://www.transitionzero.org/shedding-light-on-pakistans-distributed-solar-revolution
3. Ember & Renewables First. (2026). The solarisation of Pakistan's energy economy. Ember. https://ember-energy.org/latest-insights/the-solarisation-of-pakistans-energy-economy/

4. Renewables First. (2026). Pakistan electricity review 2026. https://uploads.renewablesfirst.org/Pakistan%20Electricity%20Review%202026.pdf

5. Sadiqa, A., Gulagi, A., & Breyer, C. (2018). Energy transition roadmap towards 100% renewable energy and role of storage technologies for Pakistan by 2050. Energy, 147, 518-533. https://doi.org/10.1016/j.energy.2018.01.027

6. Sadiqa, A., Gulagi, A., Bogdanov, D., Caldera, U., & Breyer, C. (2022). Renewable energy in Pakistan: Paving the way towards a fully renewables-based energy system across the power, heat, transport and desalination sectors by 2050. IET Renewable Power Generation, 16(1), 177-197. https://doi.org/10.1049/rpg2.12278

7. Mirjat, N. H., Uqaili, M. A., Harijan, K., Walasai, G. D., Mondal, M. A. H., & Sahin, H. (2018). Long-term electricity demand forecast and supply side scenarios for Pakistan (2015-2050): A LEAP model application for policy analysis. Energy, 165, 512-526. https://doi.org/10.1016/j.energy.2018.10.012

8. Perwez, U., Sohail, A., Hassan, S. F., & Zia, U. (2015). The long-term forecast of Pakistan's electricity supply and demand: An application of long range energy alternatives planning. Energy, 93(Part 2), 2423-2435. https://doi.org/10.1016/j.energy.2015.10.103

9. Jamal, N. (2016). A renewable electricity supply system in Pakistan by 2050: Assessment of generation capacity and transmission system requirements [Doctoral dissertation, Europa-Universität Flensburg]. https://www.zhb-flensburg.de/fileadmin/content/spezial-einrichtungen/zhb/dokumente/dissertationen/jamal/phd-thesis.pdf

10. Joyo, F. H., Groppi, D., Kumar, L., Nastasi, B., & Astiaso Garcia, D. (2025). Achieving energy sustainability of Pakistan's power sector through long-term scenario modeling and analysis. Energy, 328, 136549. https://doi.org/10.1016/j.energy.2025.136549

11. Aized, T., Shahid, M., Bhatti, A. A., Saleem, M., & Anandarajah, G. (2018). Energy security and renewable energy policy analysis of Pakistan. Renewable and Sustainable Energy Reviews, 84, 155-169. https://doi.org/10.1016/j.rser.2017.05.254

12. Kumar, R., Asim, M., Kanwal, A., Jawad, M., & Pervez, M. (2024). Toward a renewable future: Attaining 100% renewable electricity generation through sustainable transition. AIP Advances, 14(8), 085032. https://doi.org/10.1063/5.0208838

13. Raza, M. A., Aman, M. M., Rajpar, A. H., Bashir, M. B. A., & Jumani, T. A. (2022). Towards achieving 100% renewable energy supply for sustainable climate change in Pakistan. Sustainability, 14(24), 16547. https://doi.org/10.3390/su142416547

14. Abbasi, S. A., Harijan, K., Khan, M. W. A., Mengal, A., Shaikh, F., Memon, Z. A., Mirjat, N. H., & Kumar, L. (2021). Long-term optimal power generation pathways for Pakistan. Energy Science & Engineering, 9(12), 2252-2267. https://doi.org/10.1002/ese3.981

15. Gulagi, A., Choudhary, P., Bogdanov, D., & Breyer, C. (2017). Electricity system based on 100% renewable energy for India and SAARC. PLOS ONE, 12(7), e0180611. https://doi.org/10.1371/journal.pone.0180611

16. National Transmission and Despatch Company & Independent System and Market Operator. (2025). Indicative generation capacity expansion plan (IGCEP) 2025-35 (Revised, R2). National Electric Power Regulatory Authority. https://nepra.org.pk/Admission%20Notices/2025/08%20Aug/IGCEP_2025-35_R2.pdf

17. National Transmission and Despatch Company. (2024). Indicative generation capacity expansion plan (IGCEP) 2024-34. National Electric Power Regulatory Authority. https://nepra.org.pk/Admission%20Notices/2024/05%20May/IGCEP%202024-34%20Report.pdf

18. Garver, L. L. (1966). Effective load carrying capability of generating units. IEEE Transactions on Power Apparatus and Systems, PAS-85(8), 910-919. https://doi.org/10.1109/TPAS.1966.291652

19. Keane, A., Milligan, M., Dent, C. J., Hasche, B., D'Annunzio, C., Dragoon, K., Holttinen, H., Samaan, N., Söder, L., & O'Malley, M. (2011). Capacity value of wind power. IEEE Transactions on Power Systems, 26(2), 564-572. https://doi.org/10.1109/TPWRS.2010.2062543

20. Madaeni, S. H., Sioshansi, R., & Denholm, P. (2013). Comparing capacity value estimation techniques for photovoltaic solar power. IEEE Journal of Photovoltaics, 3(1), 407-415. https://doi.org/10.1109/JPHOTOV.2012.2217114

21. North American Electric Reliability Corporation. (2011). Methods to model and calculate capacity contributions of variable generation for resource adequacy planning. NERC Integration of Variable Generation Task Force. https://web.archive.org/web/20250716220922/https://www.nerc.com/pa/RAPA/ra/Reliability%20Assessments%20DL/IVGTF1-2.pdf

22. Midcontinent Independent System Operator. (2024). Wind and solar capacity credit report, planning year 2024-2025. MISO. https://cdn.misoenergy.org/Wind%20and%20Solar%20Capacity%20Credit%20Report%20PY%202024-2025632351.pdf

23. General Electric International, Inc. (2022). Evaluation of ELCC methodology in the ISO-NE footprint [Report prepared for ISO New England]. https://www.iso-ne.com/static-assets/documents/2022/10/a09b_mc_2022_10_12-13_rca_nrdc_report.pdf

24. Mirza, I. A., Khan, N. A., & Memon, N. (2010). Development of benchmark wind speed for Gharo and Jhimpir, Pakistan. Renewable Energy, 35(3), 576-582. https://doi.org/10.1016/j.renene.2009.08.008

25. Pakistan Meteorological Department. (n.d.). An investigation on wind power potential of Gharo (three years April 2002 to March 2005) [Wind Mapping Project report]. https://web.archive.org/web/20240707140730/https://www.pmd.gov.pk/wind/Sindh/Gharo.pdf

26. Dunning, C. M., Turner, A. G., & Brayshaw, D. J. (2015). The impact of monsoon intraseasonal variability on renewable power generation in India. Environmental Research Letters, 10(6), 064002. https://doi.org/10.1088/1748-9326/10/6/064002

27. Shah, R. (2024). Redirecting wind in India. Ember. https://ember-energy.org/latest-insights/redirecting-wind-in-india/

28. Hunt, K. M. R., & Bloomfield, H. C. (2024). Quantifying renewable energy potential and realized capacity in India: Opportunities and challenges. Meteorological Applications, 31(3), e2196. https://doi.org/10.1002/met.2196

29. Tong, D., Farnham, D. J., Duan, L., Zhang, Q., Lewis, N. S., Caldeira, K., & Davis, S. J. (2021). Geophysical constraints on the reliability of solar and wind power worldwide. Nature Communications, 12, 6146. https://doi.org/10.1038/s41467-021-26355-z

30. Lave, M., & Ellis, A. (2016). Comparison of solar and wind power generation impact on net load across a utility balancing area. In 2016 IEEE 43rd Photovoltaic Specialists Conference (PVSC). https://doi.org/10.1109/PVSC.2016.7749939

31. Khan, H. O. A., Tahir, M. U., Ahmad, A., & Arshad, N. (2022). Reduction in weighted average cost of generation by utilizing ToU pricing models: A study from Pakistan. In 2022 11th International Conference on Renewable Energy Research and Application (ICRERA) (pp. 119-124). IEEE. https://doi.org/10.1109/ICRERA55966.2022.9922789

32. Waleed, K. (2026, May). Pakistan's power grid development status [Presentation slides]. Sustainable Development Policy Institute; United Nations Economic and Social Commission for Asia and the Pacific. https://www.unescap.org/sites/default/d8files/event-documents/Pakistan%27s%20grid%20Khalid%20Waleed,%20SDPI.pdf

33. Independent System and Market Operator. (2025). Hourly system demand and generation data, FY2016 to FY2025 [Unpublished raw data]. National Power Control Centre.

34. National Electric Power Regulatory Authority. (2013-2026). Decisions of the Authority in the matter of fuel charges adjustment for ex-WAPDA distribution companies, October 2013 to March 2026 [Regulatory determinations; example: March 2026 decision, 5 May 2026]. https://nepra.org.pk/tariff/Tariff/Ex-WAPDA%20DISCOS/2026/TRF-100%20MFPA%20FCA%20MAR-2026%2005-05-2026%208301-18.pdf

35. Gami, D., Sioshansi, R., & Denholm, P. (2017). Data challenges in estimating the capacity value of solar photovoltaics. IEEE Journal of Photovoltaics, 7(4), 1065-1073. https://doi.org/10.1109/JPHOTOV.2017.2695328

36. Hussain, M. S., Cho, K., & Park, S. (2024). Resource adequacy and integration of renewables in light of US, EU, and Pakistan's evolving power sector. Energies, 17(20), 5051. https://doi.org/10.3390/en17205051

37. Paik, C., Chung, Y., & Kim, Y. J. (2026). Marginal capacity credit analysis for utility-scale solar and wind power: A case study in the Republic of Korea. Energies, 19(2), 540. https://doi.org/10.3390/en19020540

38. Madaeni, S. H., Sioshansi, R., & Denholm, P. (2012). Comparison of capacity value methods for photovoltaics in the Western United States (NREL/TP-6A20-54704). National Renewable Energy Laboratory. https://docs.nlr.gov/docs/fy12osti/54704.pdf

39. Frew, B., Cole, W., Sun, Y., Richards, J., & Mai, T. (2017). 8760-based method for representing variable generation capacity value in capacity expansion models (NREL/CP-6A20-68869). National Renewable Energy Laboratory. https://docs.nlr.gov/docs/fy17osti/68869.pdf

40. Munoz, F. D., & Mills, A. D. (2015). Endogenous assessment of the capacity value of solar PV in generation investment planning studies. IEEE Transactions on Sustainable Energy, 6(4), 1574-1585. https://doi.org/10.1109/TSTE.2015.2456019

41. International Renewable Energy Agency. (2025). Renewable capacity statistics 2025 [Data set]. Retrieved via Our World in Data. https://ourworldindata.org/grapher/cumulative-installed-wind-energy-capacity-gigawatts

42. Hirth, L. (2013). The market value of variable renewables: The effect of solar and wind power variability on their relative price. Energy Economics, 38, 218-236. https://doi.org/10.1016/j.eneco.2013.02.004

43. Brown, T., & Reichenberg, L. (2021). Decreasing market value of variable renewables can be avoided by policy action. Energy Economics, 100, 105354. https://doi.org/10.1016/j.eneco.2021.105354

44. Pham, A., Cole, W., & Gagnon, P. (2024). Average and marginal capacity credit values of renewable energy and battery storage in the United States power system (NREL/TP-7A40-89587). National Renewable Energy Laboratory. https://www.osti.gov/servlets/purl/2478444

45. Mills, A., & Wiser, R. (2012). Changes in the economic value of variable generation at high penetration levels: A pilot case study of California (LBNL-5445E). Lawrence Berkeley National Laboratory. https://eta-publications.lbl.gov/sites/default/files/lbnl-5445e.pdf

46. Mills, A., & Wiser, R. (2014). Strategies for mitigating the reduction in economic value of variable generation with increasing penetration levels. Lawrence Berkeley National Laboratory. https://www.osti.gov/servlets/purl/1129522/

47. Gulagi, A., Ram, M., & Breyer, C. (2020). Role of the transmission grid and solar wind complementarity in mitigating the monsoon effect in a fully sustainable electricity system for India. IET Renewable Power Generation, 14(2), 254-262. https://doi.org/10.1049/iet-rpg.2019.0603

48. Awara, S., Lynch, M., Pfenninger, S., Schell, K., Sioshansi, R., Staffell, I., Samaan, N., Tindemans, S. H., Wilson, A. L., Zachary, S., Zareipour, H., & Dent, C. J. (2020). Capacity value of solar power and other variable generation: Report of the IEEE PES Task Force on Capacity Value of Solar Power. arXiv. https://doi.org/10.48550/arXiv.2007.09015

49. Institute for Strategic Studies, Research and Analysis. (2026). Prospects of wind energy in Pakistan. ISSRA. https://issra.pk/insight/2026/prospects-of-wind-energy-in-pakistan/insight.php

50. Ghumman, M. (2023, February 24). Excessive curtailments: Wind power projects accuse NPCC of discrimination. Business Recorder. https://www.brecorder.com/news/40228144

51. FPCCI warns grid congestion threatens renewable sector. (2026, June 24). The News. https://www.thenews.pk/print/1422148-fpcci-warns-grid-congestion-threatens-renewable-sector

52. Ghumman, M. (2024, April 5). Excessive loadshedding: Nepra slaps Rs50m penalty on KE, 4 other Discos. Business Recorder. https://www.brecorder.com/news/40297355